LA-UR-77-838

CONF-770341--1

TITLE: NUMERICAL METHODS FOR TWO-DIMENSIONAL CW CHEMICAL LASER POWER CALCULATIONS

AUTHOR(S): J. D. Ramshaw
T. D. Butler

SUBMITTED TO: MIRADCOM Publication containing the proceedings of the Tri-Service Chemical Laser Symposium held at Redstone Arsenal, 1-3 March, 1977.

NOTICE
This report was prepared as an account of work sponsored by the United States Government. Neither the United States nor the United States Energy Research and Development Administration, nor any of their employees, nor any of their contractors, subcontractors, or their employees, makes any warranty, express or implied, or assumes any legal liability or responsibility for the accuracy, completeness or usefulness of any information, apparatus, product or process disclosed, or represents that its use would not infringe privately owned rights.

By acceptance of this article for publication, the publisher recognizes the Government's (license) rights in any copyright and the Government and its authorized representatives have unrestricted right to reproduce in whole or in part said article under any copyright secured by the publisher.

The Los Alamos Scientific Laboratory requests that the publisher identify this article as work performed under the auspices of the USERDA.

los alamos
scientific laboratory
of the University of California
LOS ALAMOS, NEW MEXICO 87545

An Affirmative Action/Equal Opportunity Employer

MASTER

DISTRIBUTION OF THIS DOCUMENT IS UNLIMITED

Form No. 836
St. No. 2629
1/76

UNITED STATES
ENERGY RESEARCH AND
DEVELOPMENT ADMINISTRATION
CONTRACT W-7405-ENG. 36

NUMERICAL METHODS FOR TWO-DIMENSIONAL CW CHEMICAL LASER POWER CALCULATIONS*

by

J. D. Ramshaw and T. D. Butler
Theoretical Division, Group T-3
University of California
Los Alamos Scientific Laboratory
Los Alamos, New Mexico 87545

*This work was supported by the Chemical Laser Branch of the Air Force Weapons Laboratory under Project Order 77-047, and was performed under the auspices of the U.S. Energy Research and Development Administration.

ABSTRACT

The current status of two-dimensional chemical laser modeling at Los Alamos is reviewed, with emphasis on numerical methods for coupling the radiation field to the fluid dynamics so that laser power can be calculated. The primary computational model is embodied in a two-dimensional time-dependent computer code called RICE-RAD. The RICE-RAD code was developed by incorporating radiation and lasing into the basic RICE code for transient compressible multicomponent reactive fluid flow. A steady-state solution is generated as the asymptotic limit of a time-dependent calculation in which the radiative time scale is artifically lengthened to make it comparable to the fluid dynamical and chemical time scales. This procedure generates a fully converged simultaneous solution to the coupled steady-state radiation intensity and fluid dynamics equations. Threshold, J-shifting, and cutoff are fully and automatically accounted for without the necessity of special logic and testing. Example solutions are presented to illustrate the application of the code to several existing and proposed chemical laser systems. Finally, an alternate approximate method is described for estimating laser power based on nonlasing (small-signal) vibrational distributions as input.

INTRODUCTION

For the past several years, Group T-3 of the Los Alamos Scientific Laboratory has been engaged in two-dimensional chemical laser modeling for the Air Force Weapons Laboratory. In the present paper we review the current state of our computational model and present the results of several calculations that have been performed during the last year or so. We also present a new simplified method for estimating CW laser power based on nonlasing vibrational distributions.

The fluid dynamical part of our computational model is embodied in the RICE code [1-3]. RICE is an Eulerian finite-difference computer code for calculating two-dimensional, time-dependent, compressible fluid flow. The code solves the complete Navier-Stokes equations and, hence, automatically represents such features as transverse pressure gradients and recirculation regions. A steady-state solution is generated as the asymptotic limit of a time-dependent calculation. In addition to planar flow, a variable-area capability is included that allows the quasi-two-dimensional representation of flow between plates of variable spacing. Cylindrical geometry is a special case of this variable-area capability. RICE is a multicomponent code that includes the effects of multicomponent diffusion and chemical reactions between compo-

nents (species). The number of species and chemical reactions is arbitrary within the limits imposed by computer time and storage constraints. RICE utilizes the ICE numerical technique [4-6] for performing efficient fluid dynamics calculations at all Mach numbers. Traditional explicit methods are inefficient at low Mach numbers because of the Courant sound-speed timestep stability restriction. The ICE method avoids this restriction by adopting a partially implicit formulation.

The basic RICE code does not include the effects of radiation and hence is limited to calculations of nonlasing (small signal) behavior. However, many of the questions that arise in connection with chemical lasers are essentially fluid-dynamical in nature, and the RICE code allows such questions to be addressed with a precision not possible in most other codes. For several years our work was exclusively concerned with questions of this kind. Nevertheless, it is desirable also to have the capability to estimate laser power output. For this purpose, an optics model was devised and incorporated into RICE. The resulting code, RICE-RAD, allows one to perform complete CW laser power calculations, with the radiation field fully coupled to the fluid dynamics in a self-consistent fashion.

THE RICE-RAD OPTICS MODEL

The RICE-RAD optics model is based upon the radiation-transport-theory description summarized by Emanuel [7]. The principal assumptions are (1) the lasing cavity is taken to be a Fabry-Perot resonator; (2) a Doppler line-shape is assumed, with hole burning neglected, and lasing is assumed to occur at line center; (3) rotational equilib-

rium is assumed; and (4) transverse variations in the radiation intensities are neglected. As is well known [7], assumptions (1) and (3) together imply that only a single line in each vibrational band can lase at one time. This line always occurs in the P-branch.

In order to incorporate radiation into the RICE code, two main modifications were necessary. First, the appropriate radiative terms had to be added to the lasing species continuity equations and to the internal energy equation. These terms introduce the radiation intensities I_ν into the equation system. Second, equations for the I_ν had to be added to determine these additional variables.

Because RICE is a transient code, it is natural to use the transient form of the radiation transport equation, averaged over the transverse direction. However, the radiative time scale is very short compared to the fluid dynamical and chemical time scales, a circumstance which would ordinarily require that very small timesteps be taken. To avoid the inefficiency this would entail, we artifically lengthen the radiative time scale to make it comparable to the fluid dynamical and chemical time scales. This is permissible because the coefficient that determines the radiative time scale drops out of the equations in steady state, and can therefore be arbitrarily adjusted without altering the steady state solution. With this modification, the fluid dynamics and radiation equations evolve on the same time scale and can be efficiently marched out to steady state together. The resulting equation for the I_ν is

$$\frac{\partial I_\nu}{\partial t} = a_\nu(\tau_\nu - G)I_\nu, \qquad (1)$$

where I_v is the radiation intensity in vibrational band $(v+1 \rightarrow v)$, τ_v is the corresponding gain for one pass through the system, G is the mirror loss coefficient, and a_v is the coefficient that specifies the artificial radiative time scale. According to our previous assumptions, all the intensity I_v is present in a single transition, namely the transition which maximizes τ_v. This transition is conventionally denoted by $(v + 1, J_v^* - 1) \rightarrow (v, J_v^*)$, and is identified by the rotational quantum number J_v^*.

Solving the transient Eq. (1) for the I_v has several advantages. By inspection, it is seen that in steady state either $\tau_v = G$ (the usual gain-equals-loss condition) or $I_v = 0$ (the band in question is not lasing). Thus each vibrational band is allowed to lase independently of the others, at its own value of J_v^*. Threshold and cutoff are fully and automatically accounted for without the necessity of special testing and coding logic.

Since Eq. (1) involves no spatial derivatives, a simple time-centered numerical scheme is used for its solution. The coefficient a_v is constrained by stability and by the requirement that the I_v change only slightly from one time cycle to the next. This latter requirement has the effect of making the radiative and fluid dynamical time scales approximately the same, because the timestep itself is chosen to prevent the fluid dynamical variables from changing too much over one cycle.

The above discussion is necessarily very brief and is intended only to convey the flavor and essential ideas of the RICE-RAD optics model. A detailed description of the model is available in Ref. [8]. We now proceed to show some of the results obtained in calculations using the RICE-RAD code.

NUMERICAL EXAMPLES

Our first full-scale RICE-RAD lasing calculation is a simulation of CL-V run HB5-1989 [9]. The geometry is shown schematically in Fig. 1. The region of computation is the region downstream of a typical pair of half-nozzles. The nozzle bank is composed of 115 such pairs. Similiar conditions are assumed to obtain downstream of each pair, so that the lateral boundaries (extended nozzle centerlines) are symmetry planes.

Five DF vibrational levels were included in the calculation (v = 0 to 4). Chemical reaction rate coefficients were taken from Cohen's DF compilation [10]. Initially 56 reactions were included in an effort to model the important deactivation reactions. DF-DF V-V transfer was included, but vibrational levels of D_2 were not represented and hence DF-D_2 V-V transfer reactions were not included. We later reran the calculation with the number of reactions reduced to 16, omitting most of the backward reactions and all the DF-DF V-V transfer reactions; the results were essentially unchanged.

Nozzle exit plane boundary conditions for the calculation were obtained from M. C. Cline of our group, who performed the necessary viscous nozzle calculations using his VNAP code [11]. (Cline's VNAP code is unrelated to the TRW VNAP code.) The nozzle calculations did not include chemistry, and mass fractions of the various species at the nozzle exit plane were taken to be uniform. Thus F-atom recombination at the nozzle walls was neglected.

Figure 2 shows the velocity vector plot for the region $0 \leq x \leq 0.45$ cm. The scale is such that the largest velocity in the region is about 2.5×10^5 cm/s. Since the CL-V nozzles are uniformly flared, the velocity in the nozzle exit plane has a transverse

component. The transverse momentum density in the fluorine stream is considerably larger than that in the deuterium stream, so that the deuterium is compressed by the expanding fluorine stream.

Figure 3 shows the pressure contour plot in the same region, $0 \leq x \leq 0.45$ cm. Note the presence of substantial transverse pressure gradients in this region, even though the nozzle exit pressures are matched to within a few percent.

The pressure contour plot for the region $3.05 \text{ cm} \leq x \leq 4.55$ cm is shown in Fig. 4. Here the pressure variations are much weaker in magnitude. The most noteworthy feature of the plot, however, is that the pressure contours form a regular pattern of alternating high and low pressure islands. This pattern is symptomatic of the reflections of Mach waves at the top and bottom symmetry boundaries. By inspection, the wavelength for this pattern is about 1 cm, which correlates very closely with the wavelength one would predict on the basis of the Mach angle and the height of the region. These Mach waves have an interesting effect on the laser power profile, as will be seen shortly.

Figure 5 shows transverse profiles of the molar densities of D_2, F, and total DF at $x = 4.0$ cm. From this plot it is clear that the system is very D_2 rich. The small area of overlap of the D_2 and F streams in comparison with the DF area shows that the production of DF is primarily mixing limited rather than chemistry limited.

This implies that the calculation as a whole should be relatively insensitive to the overall cold reaction rate coefficient (but not to the pumping fractions). This insensitivity has been confirmed by Zelazny et al. [13].

Figure 6 shows transverse profiles of the DF vibrational levels at x = 4.0 cm. The profiles have maxima in the mixing layer, where the DF is being produced, and their relative peak values reflect a typical partial inversion in the presence of lasing.

The power profile for the calculation is shown in Figure 7. The quantity plotted is the power per unit length, the integral of which gives the total power. The most noteworthy feature of the curve are the sharp peaks. Inspection shows that the peaks occur in groups of two with a spacing of about 1 cm between adjacent groups. These peaks are correlated with, and in fact caused by, the Mach waves mentioned earlier. Wherever the Mach wave intersects the mixing layer, the rate of production of DF is locally enhanced due to the associated compression and heating. The intersection occurs twice per wavelength, which is why the peaks occur in groups of two. The spacing between the two peaks in a group is somewhat different from half the wavelength because the mixing layer is not exactly centered between the symmetry boundaries. Because it involves oblique shock waves and transverse pressure gradients in an essential way, this effect cannot be described in the boundary layer approximation. Experimentally, these power peaks are not observed because the use of a hemispherical mirror has the effect of averaging the power profile over x. However, the Mach waves are still present, thereby enhancing the local DF production and the <u>total</u> power.

In the present calculation, the calculated total power is higher than the experimental value by approximately a factor of two. Part of this discrepancy is due to the fact that we inadvertently set the spectroscopic constant $\omega_e x_e$ to zero. If this error had not been made the calculated power would have been about 13 kW, which is still too high. However, this agreement is considered satisfactory in view of the omission of a number of potentially important effects from the calculation. Among the most important of these are (1) F-atom wall recombination; (2) DF-D_2 V-V transfer; and (3) rotational nonequilibrium. Other uncertainties include (1) the effect of the hemispherical mirror; (2) three-dimensional effects associated with the shroud expansion and boundary layers; and (3) uncertainties in diffusion coefficients and reaction rate coefficients, in particular the modeling of multiquantum deactivation in terms of effective single-quantum deactivation rates.

The basic CL-V calculation just described was rerun in cylindrical coordinates to simulate a hypothetical CL-V cylindrical laser. The diameter of the cylindrical nozzle bank was taken to be 46 cm. The equivalent shroud expansion half-angle for the one-inch-high CL-V nozzle bank is 3° (neglecting shroud boundary layers). In spite of this small angle, relatively large effects were observed. The pressure on the line y = 0.119 cm is plotted vs. x for both the rectangular and cylindrical cases in Fig. 8. The cylindrical expansion provides considerable pressure relief; at x = 8 cm the pressure in the cylindrical case is only about 14 torr and is rising very slowly, while in the rectangular case, the pressure is about 25 torr and is climbing at a rate of about 2 torr/cm. A similar effect is seen in Fig. 9, which shows the maximum temperature

on a line of constant x versus x for the two cases. The cylindrical temperature is considerably less than the rectangular (by almost 90°K at x = 8 cm) due to the expansion. Finally, the power profiles for the two cases are compared in Fig. 10. The cylindrical profile is normalized to the same mass flow rate as in the rectangular case, and $\omega_e x_e$ was again set equal to zero to facilitate the comparison. The two power profiles are essentially identical out to about 3 cm, but begin to differ noticeably thereafter. Cutoff occurs considerably farther downstream in the cylindrical case, and the total power is about 33% higher than in the rectangular case.

We now describe briefly a chain reaction laser calculation performed using RICE-RAD. The calculation was performed for HF lasing using the Rocketdyne baseline nozzle array. The fluorine dissociation fraction was $\alpha = 0.1$ and the diluent ratio was $\beta = 60$. The diluent was helium and was present only in the fluorine nozzle. The large value of β was necessary to prevent choking. The first seven vibrational levels of HF were considered (v = 0 to 6). Vibrational levels of H_2 were not included. Both hot and cold reactions were included, and the chemical reaction rate coefficients were obtained primarily from Cohen's latest HF compilation [14]. However, the inverse cold reaction rates for $v \geq 3$ were increased in an attempt to allow for the large removal rate of HF(3) by H atoms observed by Bott and Heidner [15]. A total of 29 chemical reactions was included in the calculation.

Figure 11 shows the maximum temperature on a line of constant x plotted versus x. The maximum temperature starts out high because of viscous heating at the nozzle walls, falls off sharply to a low value of about 220°K which persists down to about x = 25 cm, and then begins

to rise rapidly as the chain reaction finally begins to "take off". The power profile for the calculation is shown in Fig. 12. There is a peak in the high-temperature region near the nozzle exit plane, but the power falls off sharply, and then more gradually, to a minimum at about x = 23 cm. The power then begins to increase with x, in a nearly linear fashion, as the chain reaction proceeds. The calculation was arbitrarily terminated at x = 50 cm, on the ground that it is probably not reasonable to contemplate using larger mirrors than that. The specific power out to this point is σ = 46.1 kJ/lb. However, the power profile is still increasing at this point, and if the calculation were continued farther downstream it appears that considerable additional power would be obtained. In fact, only 27% of the incoming fluorine has reacted by x = 50 cm. If the same basic fluorine efficiency could be maintained until all the fluorine is gone, a specific power of about 170 kJ/lb would result. Of course, to achieve this result in a practical configuration, it would also be necessary to vary the flow conditions in a way that would considerably shorten the lasing zone without seriously altering the efficiency.

ALTERNATE OPTICS MODEL

We now describe an approximate alternative method for estimating laser power based on non-lasing (small-signal) vibrational distributions as input. This method is a further refinement of the approximate steady-state lasing prescription described in Section 4 of Reference [8]. The new method differs from the earlier one in the way in which the power is calculated once the lasing population densities have been obtained. The new power calculation is less exact than the earlier one, but it is much simpler and easier to implement.

There are several reasons why an approximate method of this kind is of interest. If a steady-state calculation without lasing has already been performed, one would like to be able to estimate the corresponding laser power simply and quickly without performing another complete steady-state calculation with lasing. The present method provides a means of doing so. Another motivation for considering such an approximate method is that the basic RICE-RAD method already described does not work well at high pressures ($p \gtrsim 0.3$ atm). The system of coupled radiation intensity and lasing species equations appears to become very stiff and convergence difficulties are experienced. The approximate method avoids this difficulty by reformulating the problem so that the determination of the lasing species populations is essentially uncoupled from the determination of the radiation intensities.

The approximate method for estimating CW laser power depends upon the fact that the basic fluid dynamical variables are essentially the same whether the system is lasing or not. This may at first appear surprising, because when the system is lasing the radiation field removes energy which would otherwise be released as heat. However, this effect is relatively small, because typical chemical laser efficiencies are on the order of 10% or less. Thus even when the system is lasing, roughly 90% of the chemical energy is still released as heat, and the difference in temperature between the lasing and non-lasing cases is consequently small. One might worry that even a small temperature difference could produce a large effect because of the very strong temperature-dependence of the chemical reaction rate coefficients. This potential effect is largely ameliorated by the fact that the diffusion-type lasers of interest

here are primarily mixing-limited rather than chemistry limited. Thus the primary effect of lasing is to redistribute the lasing species vibrational populations, and the effect of lasing on the primary fluid dynamical variables may be neglected to a first approximation.

Another simplification that the approximate method utilizes is that the vibrational populations in the presence of lasing are only weakly dependent on the actual values of the radiation intensities. It is this fact which allows the determination of the lasing species distribution to be uncoupled from the determination of the radiation intensities and power. The lasing species populations are determined by the gain-equals-loss condition, together with a reasonable assumption about the distribution of the total gain in the transverse direction. The resulting expression for the vibrational populations in the presence of lasing is given by Eq. (50) of Ref. [8]. This expression is a generalization of one given by Emanuel and Whittier [16]. The equation is most easily discussed in the closed-cavity limit, in which it takes the particularly simple form

$$\rho_v = \frac{B^v(1-B)}{1-B^{NV}} \sum_{\ell} \rho_{\ell}^o \quad , \tag{2}$$

where ρ_v^o is the nonlasing partial density of level v, ρ_v is the partial density of level v when the system is lasing, NV is the total number of vibrational levels being considered (including the ground state), and

$$B = \exp\{-2J^* \theta_r / T\} \quad , \tag{3}$$

where θ_r is the characteristic rotational temperature of the lasing species, T is the absolute temperature, and J^* is the value of the rotational quantum number for which the maximum gain occurs. In contrast to the more exact RICE-RAD method, a single value of J^* is used here for all vibrational bands. Since J^* depends on the ρ_v, B is an implicit function of the ρ_v and Eqs. (2) and (3) must be solved simultaneously for the ρ_v. This is conveniently done by iteration. First J^* is evaluated from the ρ_v^o to determine a first guess for B. This B then determines a first guess for the ρ_v from Eq. (2). These ρ_v then determine a new J^* and hence a second guess for B, and so on. This procedure converges rapidly, with 10 to 20 iterations typically being sufficient. However, special care must be taken at high pressures because of the sensitivity previously mentioned. A procedure which works well is to initialize J^* to its minimum possible value (one) at the start of the calculation, allow it to increase at a rate of at most one per iteration, and not allow it to decrease. In this way J^* approaches its final value gradually from below. This procedure also prevents the cyclic behavior alluded to in Sect. 4 of Ref. [8], which sometimes caused J^* to alternate between two adjacent values even in low-pressure problems.

Since we are concerned with a two-dimensional description, the ρ_v are functions of both the longitudinal distance x and the transverse distance y. They must be determined by a local application of the preceding formulas at each point (x,y) in the lasing cavity. J^*, however, is a function of x alone, but a functional of the y-dependence of the ρ_v.

The procedure described above for determining the lasing species populations ρ_v from the ρ_v^o is the same as that described in Sect. 4 of Ref. [8]. However, the laser power is now calculated from the ρ_v in a new and simplier way. Actually two new approximate power formulas have been developed. The simplest and least accurate formula is

$$P(x) = \frac{Nh}{M} \sum_{v=1}^{NV-1} \left(\sum_{\ell=0}^{v-1} \nu_\ell \right) [\rho_v^o(x) - \rho_v(x)] u(x) A(x), \qquad (4)$$

where $P(x)$ is the integrated power from the nozzle exit plane ($x=0$) to the downstream point x, N is Avogadro's number, h is Planck's constant, M is the molecular weight of the lasing species, ν_v is the spectral frequency of the transition $(v+1, J^*-1) \rightarrow (v, J^*)$, $u(x)$ is the velocity, and $A(x)$ is the variable area function. For simplicity, Eq. (4) and the following equations are written in one-dimensional variable-area form, but the generalization to two dimensions is straightforward and it is the two-dimensional formulation that we actually use. Equation (4) has a simple intuitive interpretation: it attributes the laser power in the region upsteam of x to the difference between the vibrational energy per unit time leaving the system in the nonlasing case (which involves the ρ_v^o) and that in the lasing case (which involves the ρ_v). The main error in this assumption is that it implicitly neglects the difference in deactivation rates between the lasing and nonlasing cases. In reality, however, the deactivation rates are less in the lasing case (because the populations of the higher levels are less) and Eq. (4) therefore underestimates the power.

A better formula, which accounts for the differences in deactivation rates between the lasing and non-lasing cases, is the following:

$$P(x) = P_1(x) + P_2(x), \tag{5}$$

$$P_1(x) = \frac{Nh}{M}\sum_{v=1}^{NV-1}\left(\sum_{\ell=0}^{v-1}\nu_\ell\right)[\hat{\beta}_v(x) - \rho_v(x)]u(x)A(x), \tag{6}$$

$$P_2(x) = -\frac{Nh}{M}\sum_{v=1}^{NV-1}\nu_{v-1}\int_0^x dx'A(x')\rho_v(x')S_v(x'), \tag{7}$$

where the $\hat{\beta}_v$ are nonlasing population densities in the absence of deactivation, related to the pumping fractions p_v by

$$\hat{\beta}_v = p_v\sum_\ell \rho_\ell^o, \tag{8}$$

and S_v is the specific deactivation rate of level v, given by

$$S_v = \sum_\alpha \frac{k_\alpha^v \rho_\alpha}{M_\alpha}, \tag{9}$$

where the sum is over all deactivating species α and k_α^v is the reaction rate coefficient for deactivation of level v by species α. The above expressions assume that only single-quantum deactivation is occurring. These equations also have a simple intuitive interpretation. The first term, $P_1(x)$, is of the same form as Eq. (4) with ρ_v^o replaced by $\hat{\beta}_v$. Thus $P_1(x)$ has the interpretation of the laser power in the region upstream of x if there were no deactivation whatever. This

overestimates the actual laser power. To correct for deactivation one must add the second contribution $P_2(x)$, which is seen to be negative. This term represents the rate of conversion of vibrational energy to heat due to deactivation in the region upstream of x when the system is lasing.

By considering the nonlasing continuity equations for the ρ_v in the presence and in the absence of deactivation, one can reexpress $S_v(x)$ in the following more convenient form:

$$S_v(x) = -\frac{1}{\rho_v^o(x)A(x)} \sum_{\ell=0}^{v-1} \frac{\partial}{\partial x} \{[\rho_\ell^o(x) - \beta_\ell(x)]u(x)A(x)\} , \qquad (10)$$

which expresses $S_v(x)$ in terms of the known quantities ρ_v^o and β_v, eliminating the explicit dependence on the rate coefficients k_α^v. Thus Eqs. (5), (6), (7), (8), and (10) enable one to estimate the laser power using only the nonlasing population densities ρ_v^o as input, without assuming specific forms for the k_α^v. These equations can therefore also be used to process <u>experimental</u> nonlasing data, provided that <u>all</u> the ρ_v^o (including the ground state) are measured. Although these equations are strictly applicable only when multiquantum deactivation is absent, we expect that they will still provide a useful approximation whenever it is possible to represent multiquantum deactivation in terms of <u>effective</u> single-quantum deactivation rates.

As previously remarked, the procedure by which the lasing populations ρ_v are computed from the nonlasing populations ρ_v^o in this method assumes that all vibrational bands are simultaneously lasing. Threshold and cut-

off are therefore not specifically allowed for in the formulation. By forcing a transition to lase whose gain is below threshold, one obtains a negative contribution to the total power. When these negative contributions begin to overshadow the positive contributions, P(x) will begin to decrease with increasing x. A reasonable guide to lasing cutoff is to locate the point at which $\partial P/\partial x$ first becomes negative, and to identify P(x) at this point with the total laser power.

It should be emphasized that the improved approximate power formula, embodied in Eqs. (5), (6), (7), (8), and (10), is restricted in its present form to cold reaction lasers, where the pumping fractions p_v can be unambiguously defined. The simpler approximate formula of Eq. (4), however, can be applied equally well to chain reaction lasers.

The method just described has so far received only a limited amount of proof-testing. We have applied it to the region $0 \leq x \leq 0.375$ cm of CL-V HB5-1989, using the more exact RICE-RAD calculation as a standard of comparison. The simplest formula, Eq. (4) above, yielded a total power for this region 7% below the RICE-RAD value. The improved formula embodied in Eqs. (5), (6), (7), (8), and (10) reduced the discrepancy to about 2%. This agreement is not surprising in view of the fact that all bands are simultaneously lasing and multiquantum deactivation is absent in this particular test problem. We have not yet tested the method over the full lasing cavity, up to and including cutoff. We hope to present a more detailed derivation of the method together with more detailed test calculations in a future publication.

REFERENCES

1. W. C. Rivard, T. D. Butler, and O. A. Farmer, "The Transient Dynamics of Chemically Reactive Gaseous Mixtures with Turbulence," Proceedings of the Fourth International Conference on Numerical Methods in Fluid Dynamics, University of Colorado, June 24-28, 1974 (Springer-Verlag, 1975), p. 334.

2. W. C. Rivard, O. A. Farmer, and T. D. Butler, "RICE: A Computer Program for Multicomponent Chemically Reactive Flows at All Speeds," Los Alamos Scientific Laboratory report LA-5812, March 1975.

3. T. D. Butler and P. J. O'Rourke, "A Numerical Method for Two Dimensional Unsteady Reacting Flows," presented at the Sixteenth (International) Symposium on Combustion, Massachusetts Institute of Technology, August 15-20, 1976.

4. F. H. Harlow and A. A. Amsden, "Numerical Calculation of Almost Incompressible Flow," J. Comp. Phys. 3, 80 (1968).

5. F. H. Harlow and A. A. Amsden, "A Numerical Fluid Dynamics Calculation Method for All Flow Speeds," J. Comp. Phys. 8, 197 (1971).

6. F. H. Harlow, A. A. Amsden, and C. W. Hirt, "Numerical Calculation of Fluid Flows at Arbitrary Mach Number," Proceedings of the Second International Conference on Numerical Methods in Fluid Dynamics, University of California (Berkeley), September 15-19, 1970 (Springer-Verlag, 1971) p. 447.

7. G. Emanuel, J. Quant. Spectrosc. Radiat. Transfer 11, 1481 (1971).

8. J. D. Ramshaw, R. C. Mjolsness, and O. A. Farmer, J. Quant. Spectrosc. Radiat. Transfer 17, 149 (1977).

9. D. L. Hook et al., "HF/DF Chemical Laser Technology Studies," AFWL-TR-74-150 (1974).

10. N. Cohen, "A Brief Review of Rate Coefficients for Reactions in the D_2-F_2 Chemical System," Aerospace Corporation, TR-0074(4530)-9 (1974); also private communications (1975).

11. M. C. Cline, AIAA J. 14, 295 (1976).

12. O. A. Farmer and J. D. Ramshaw, J. Comp. Phys. (in press).

13. S. W. Zelazny et al., AIAA paper 77-63, also this symposium.

14. N. Cohen and J. F. Bott, "A Review of Rate Coefficients in the H_2-F_2 Chemical Laser System," Aerospace Corporation, SAMSO-TR-76-82 (1976).

15. J. F. Bott and R. F. Heidner, III, this symposium.

16. G. Emanuel and J. S. Whittier, Appl. Optics 11, 2047 (1972).

REFERENCES

1. W. C. Rivard, T. D. Butler, and O. A. Farmer, "The Transient Dynamics of Chemically Reactive Gaseous Mixtures with Turbulence," Proceedings of the Fourth International Conference on Numerical Methods in Fluid Dynamics, University of Colorado, June 24-28, 1974 (Springer-Verlag, 1975), p. 334.

2. W. C. Rivard, O. A. Farmer, and T. D. Butler, "RICE: A Computer Program for Multicomponent Chemically Reactive Flows at All Speeds," Los Alamos Scientific Laboratory repor LA-5812, March 1975.

3. T. D. Butler and P. J. O'Rourke, "A Numerical Method for Two Dimensional Unsteady Reacting Flows," presented at the Sixteenth (International) Symposium on Combustion, Massachusetts Institute of Technology, August 15-20, 1976.

4. F. H. Harlow and A. A. Amsden, "Numerical Calculation of Almost Incompressible Flow," J. Comp. Phys. 3, 80 (1968).

5. F. H. Harlow and A. A. Amsden, "A Numerical Fluid Dynamics Calculation Method for All Flow Speeds," J. Comp. Phys. 8, 197 (1971).

6. F. H. Harlow, A. A. Amsden, and C. W. Hirt, "Numerical Calculation of Fluid Flows at Arbitrary Mach Number," Proceedings of the Second International Conference on Numerical Methods in Fluid Dynamics, University of California (Berkeley), September 15-19, 1970 (Springer-Verlag, 1971) p. 447.

7. G. Emanuel, J. Quant. Spectrosc. Radiat. Transfer 11, 1481 (1971).

8. J. D. Ramshaw, R. C. Mjolsness, and O. A. Farmer, J. Quant. Spectrosc. Radiat. Transfer 17, 149 (1977).

9. D. L. Hook et al., "HF/DF Chemical Laser Technology Studies," AFWL-TR-74-150 (1974).

10. N. Cohen, "A Brief Review of Rate Coefficients for Reactions in the D_2-F_2 Chemical System," Aerospace Corporation, TR-0074(4530)-9 (1974); also private communications (1975).

11. M. C. Cline, AIAA J. 14, 295 (1976).

12. O. A. Farmer and J. D. Ramshaw, J. Comp. Phys. (in press).

13. S. W. Zelazny et al., AIAA paper 77-63, also this symposium.

14. N. Cohen and J. F. Bott, "A Review of Rate Coefficients in the H_2-F_2 Chemical Laser System," Aerospace Corporation, SAMSO-TR-76-82 (1976).

15. J. F. Bott and R. F. Heidner, III, this symposium.

16. G. Emanuel and J. S. Whittier, Appl. Optics 11, 2047 (1972).

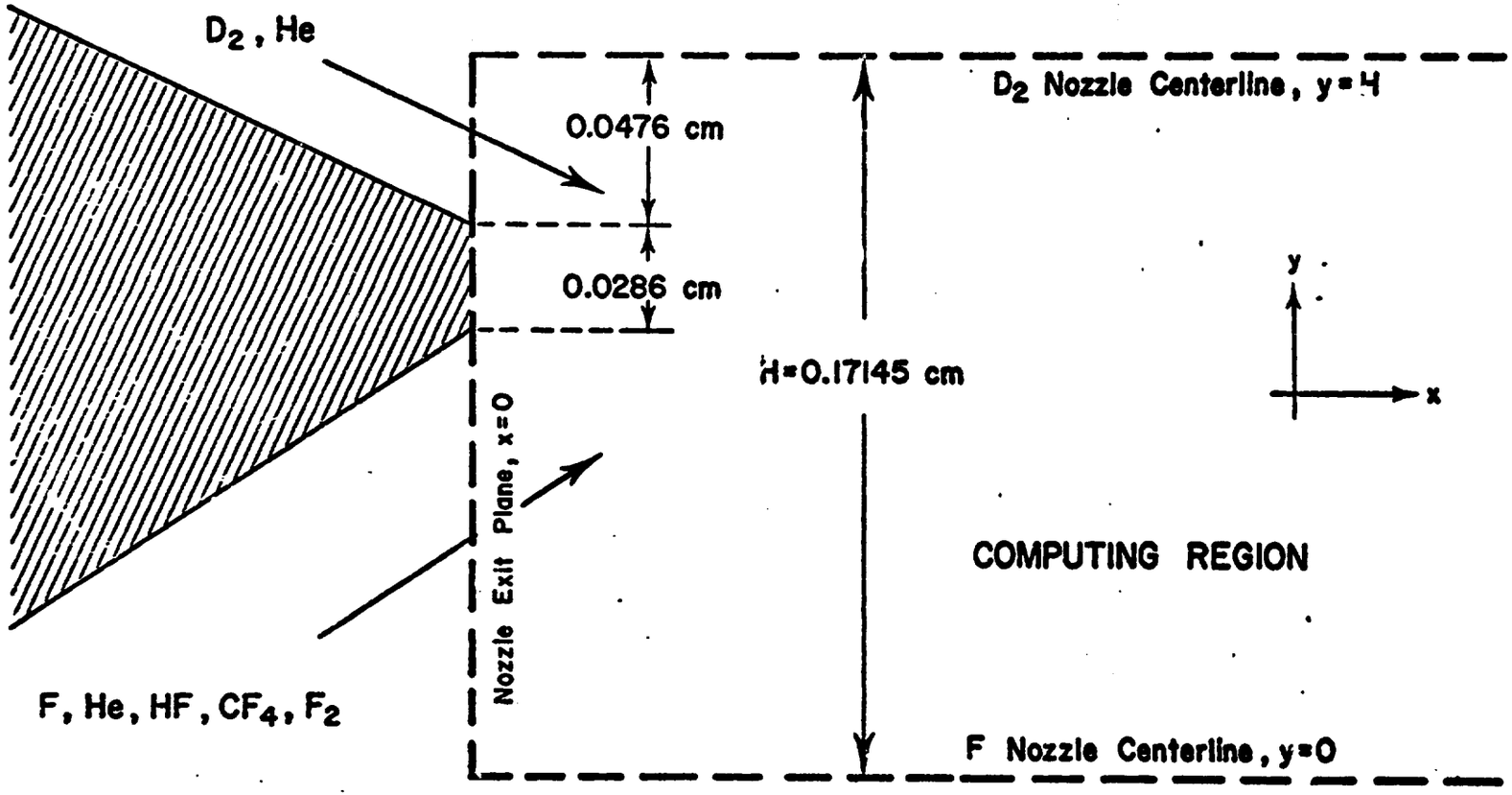

Fig. 1. Schematic diagram of computing region for CL-V calculations.

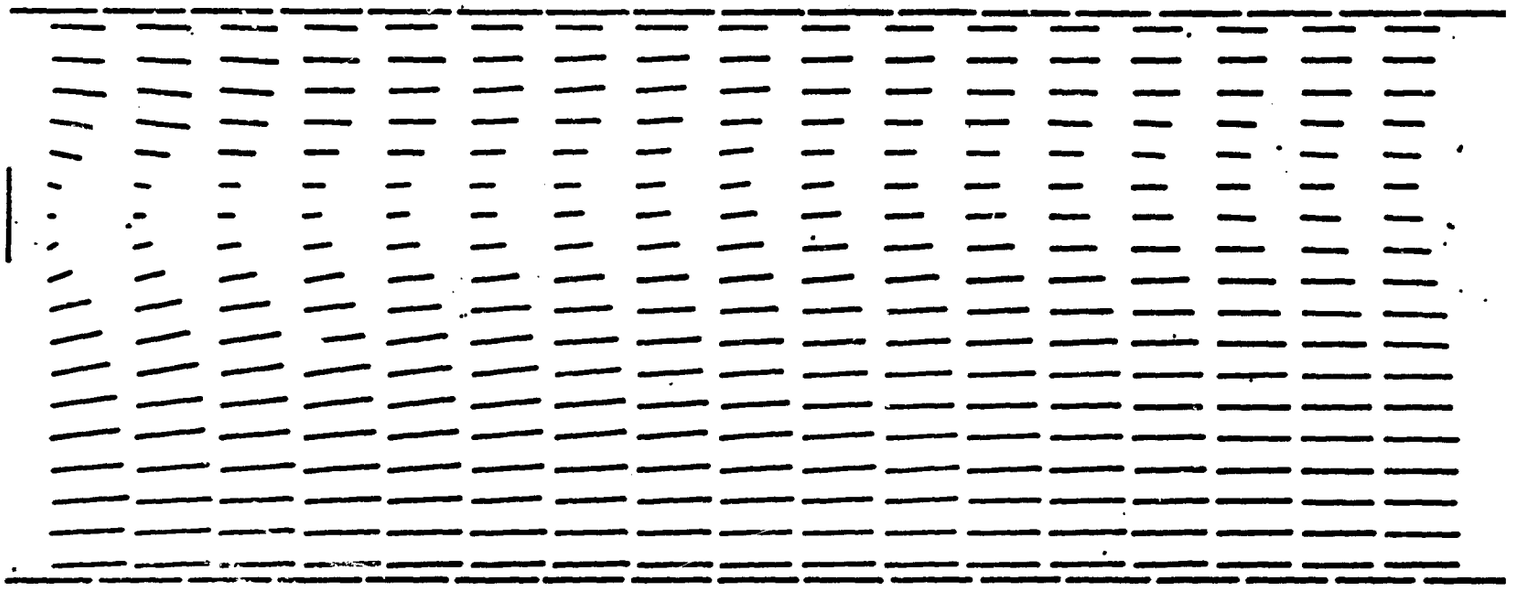

Fig. 2. Velocity vector plot for CL-V HB5-1989, x = 0 to x = 0.45 cm.

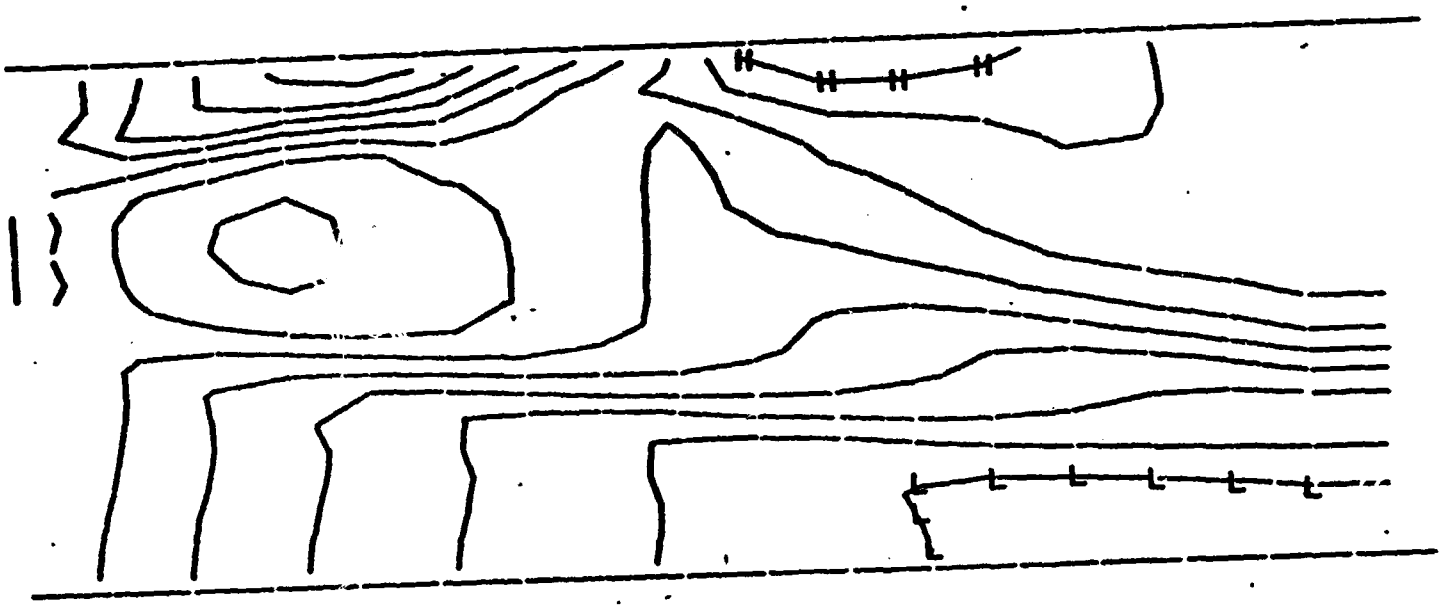

Fig. 3. Pressure contours for CL-V HB5-1989, x = 0 to x = 0.45 cm. Maximum and minimum pressures in this interval are 23.2 torr and 5.73 torr, respectively. The H contour line is 21.4 torr and the L contour line is 7.47 torr. The difference between adjacent contour lines is 1.75 torr.

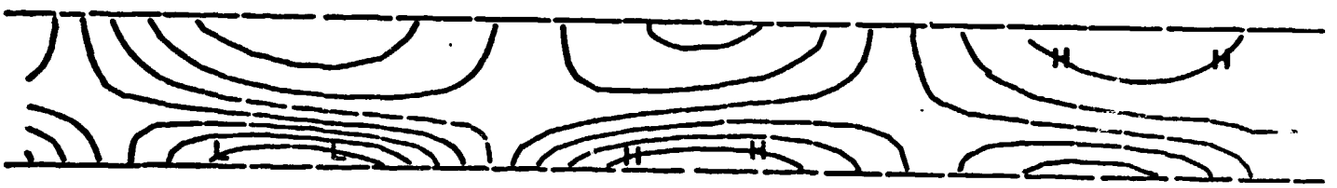

Fig. 4. Pressure contours for CL-V HB5-1989, x = 3.05 cm to x = 4.55 cm. Maximum and minimum pressures in this interval are 19.5 torr and 15.3 torr, respectively. The H contour line is 19.1 torr and the L contour line is 15.7 torr. The difference between adjacent contour lines is 0.423 torr.

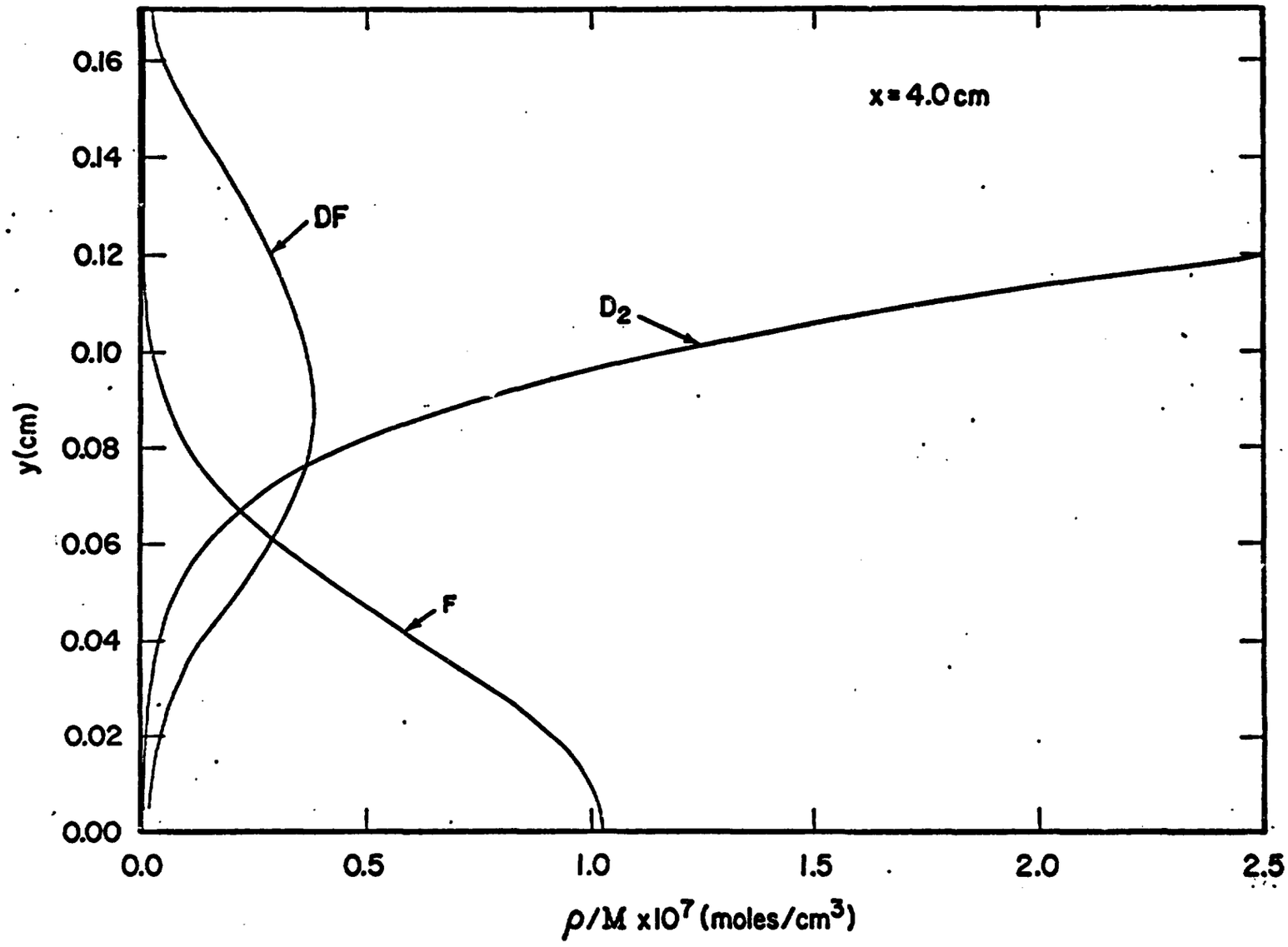

Fig. 5. Transverse profiles of molar densities of F, D_2, and total DF for CL-V HB5-1989 at x = 4.0 cm.

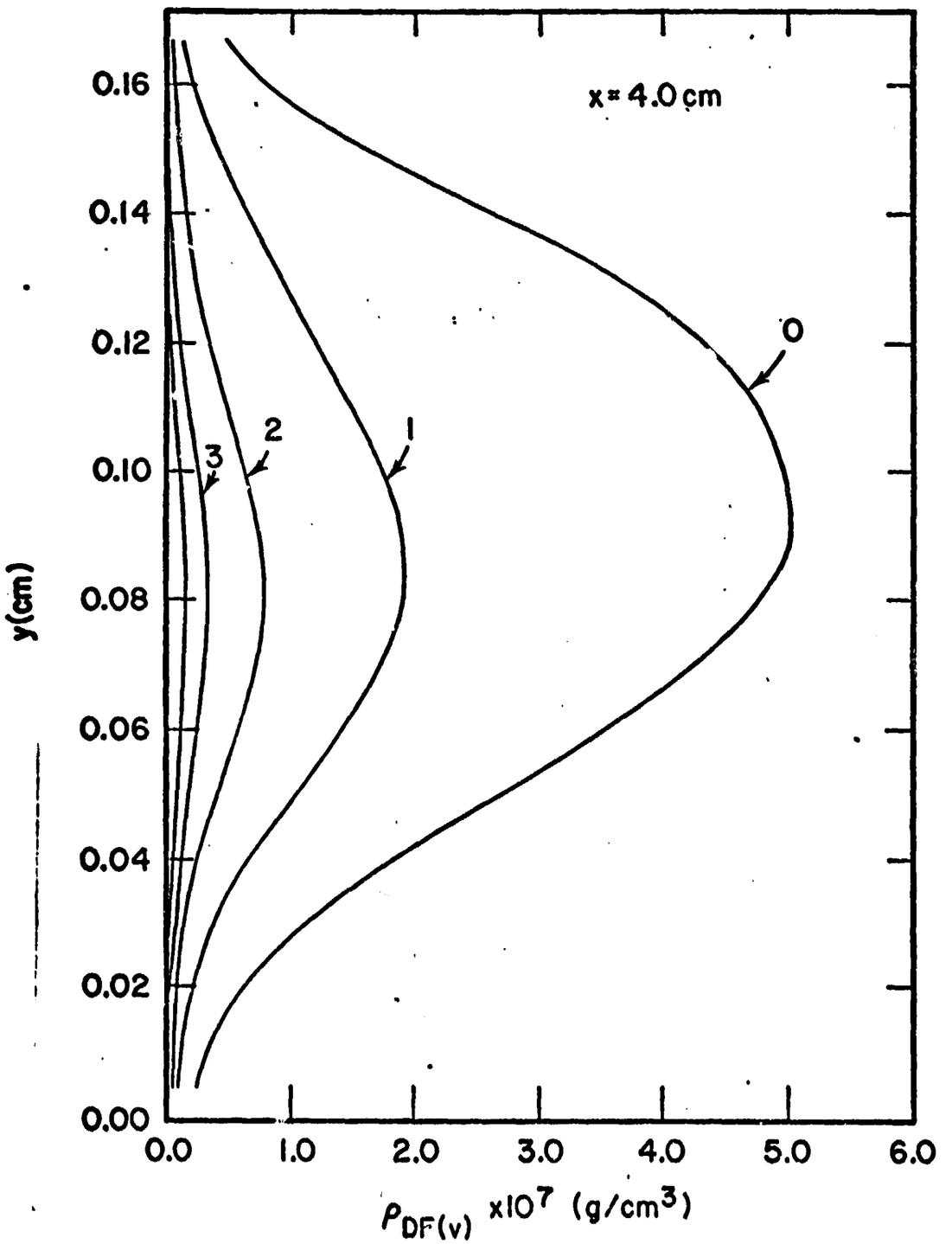

Fig. 6. Transverse profiles of mass densities of DF(v) for v = 0, 1, 2, 3, and 4 for CL-V HB5-1989 at x = 4.0 cm. The unlabeled curve is v = 4.

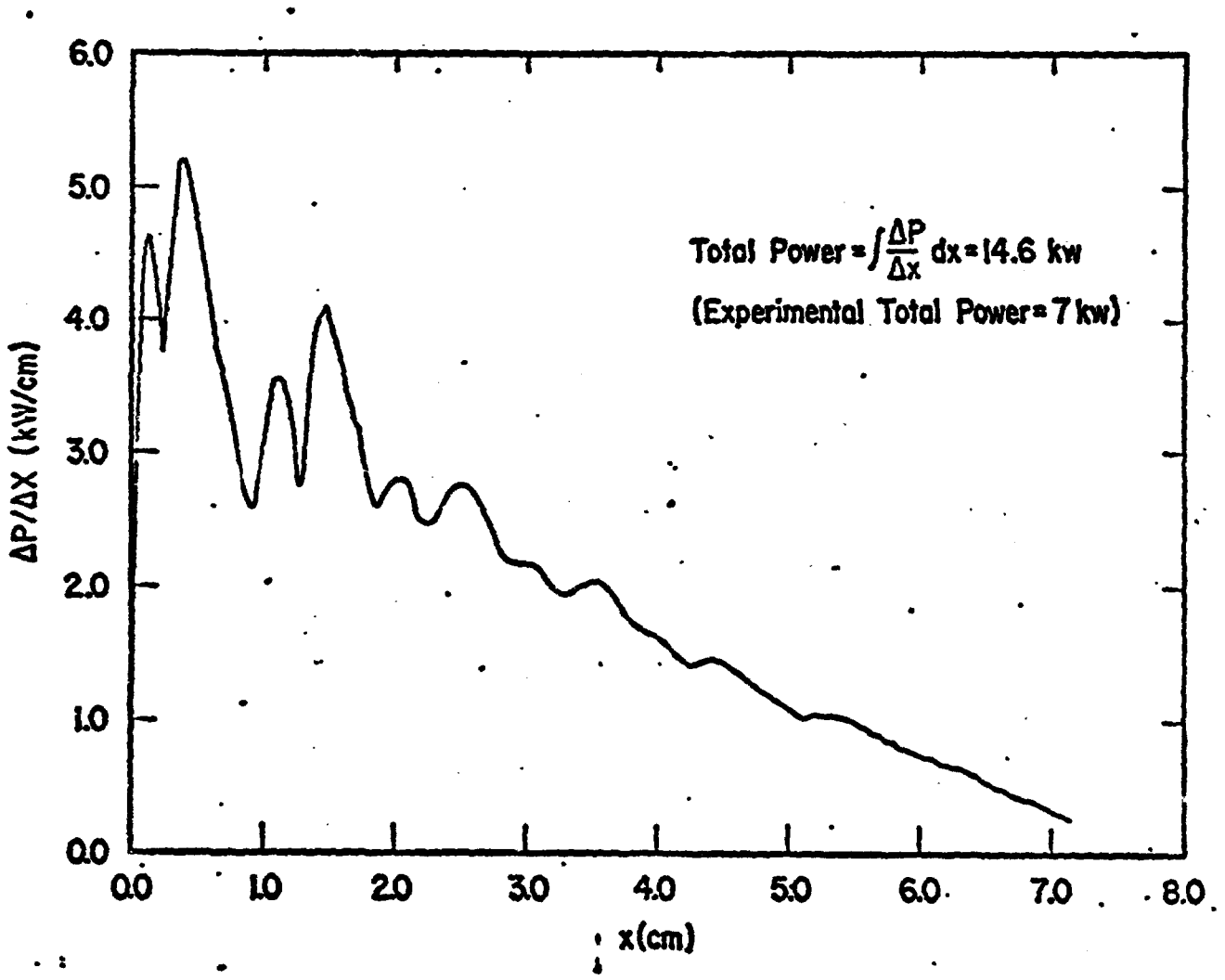

Fig. 7. Power profile for CL-V HB5-1989 with $\omega_e x_e = 0$.
x is distance from the nozzle exit plane.

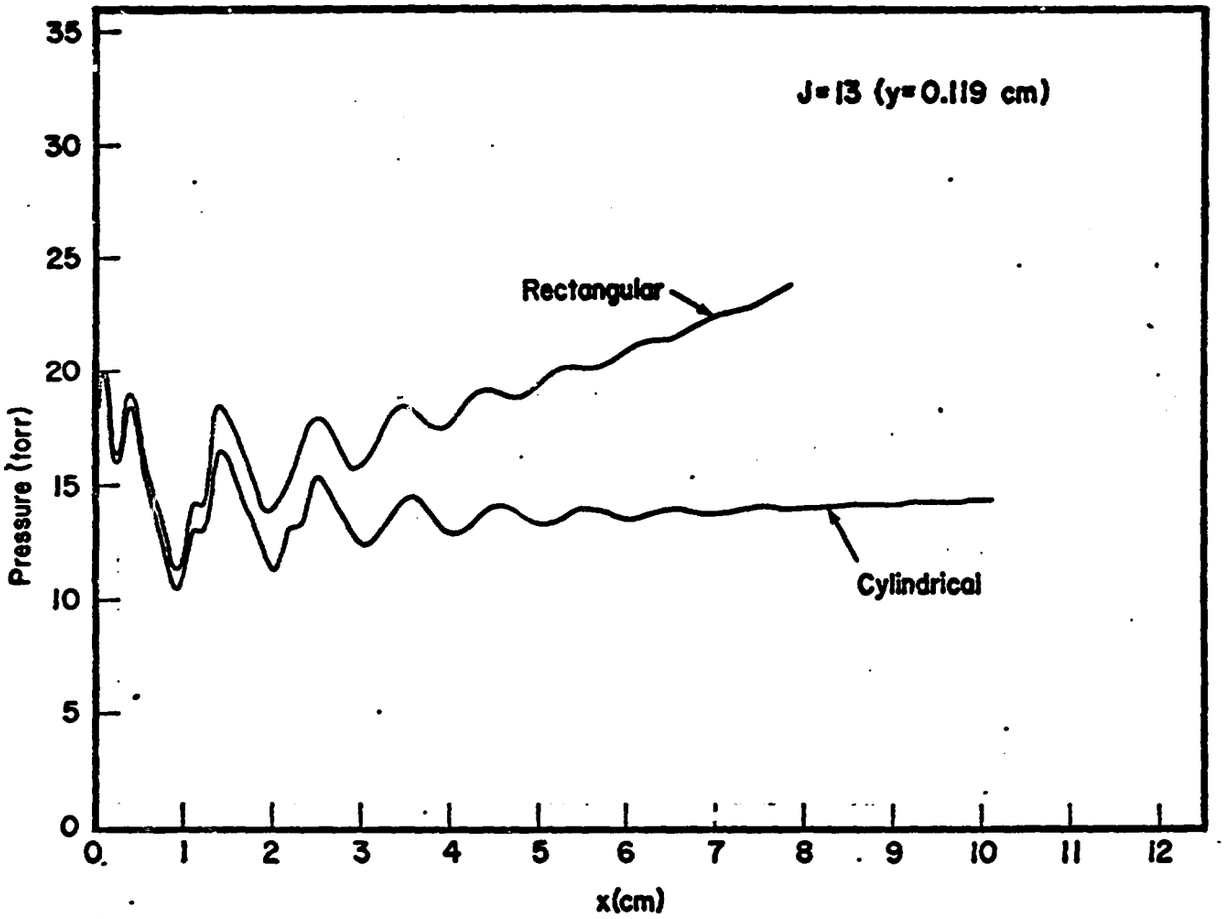

Fig. 8. Rectangular and cylindrical pressures at y = 0.119 cm vs x.

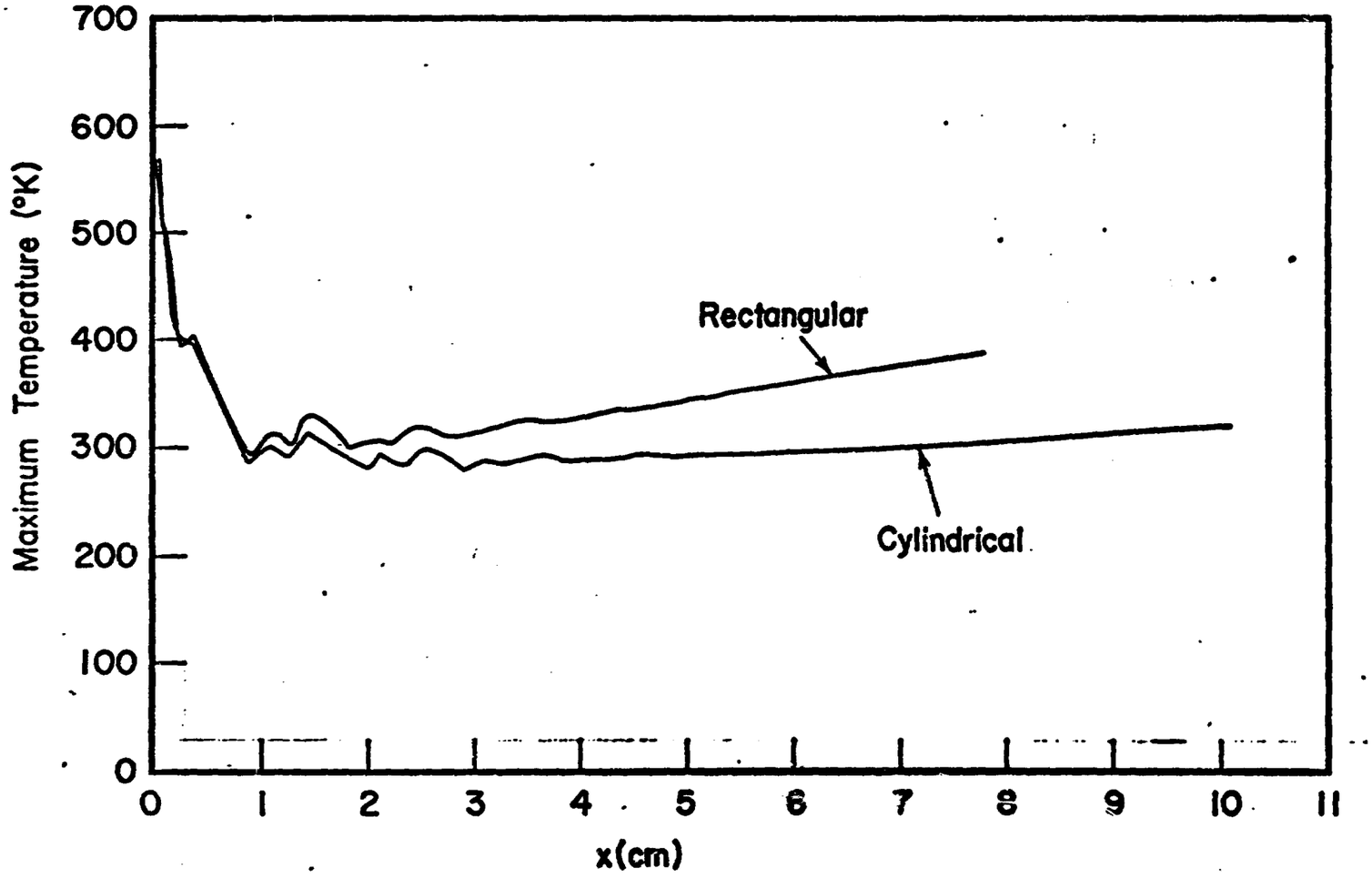

Fig. 9. Rectangular and cylindrical maximum temperatures vs x.

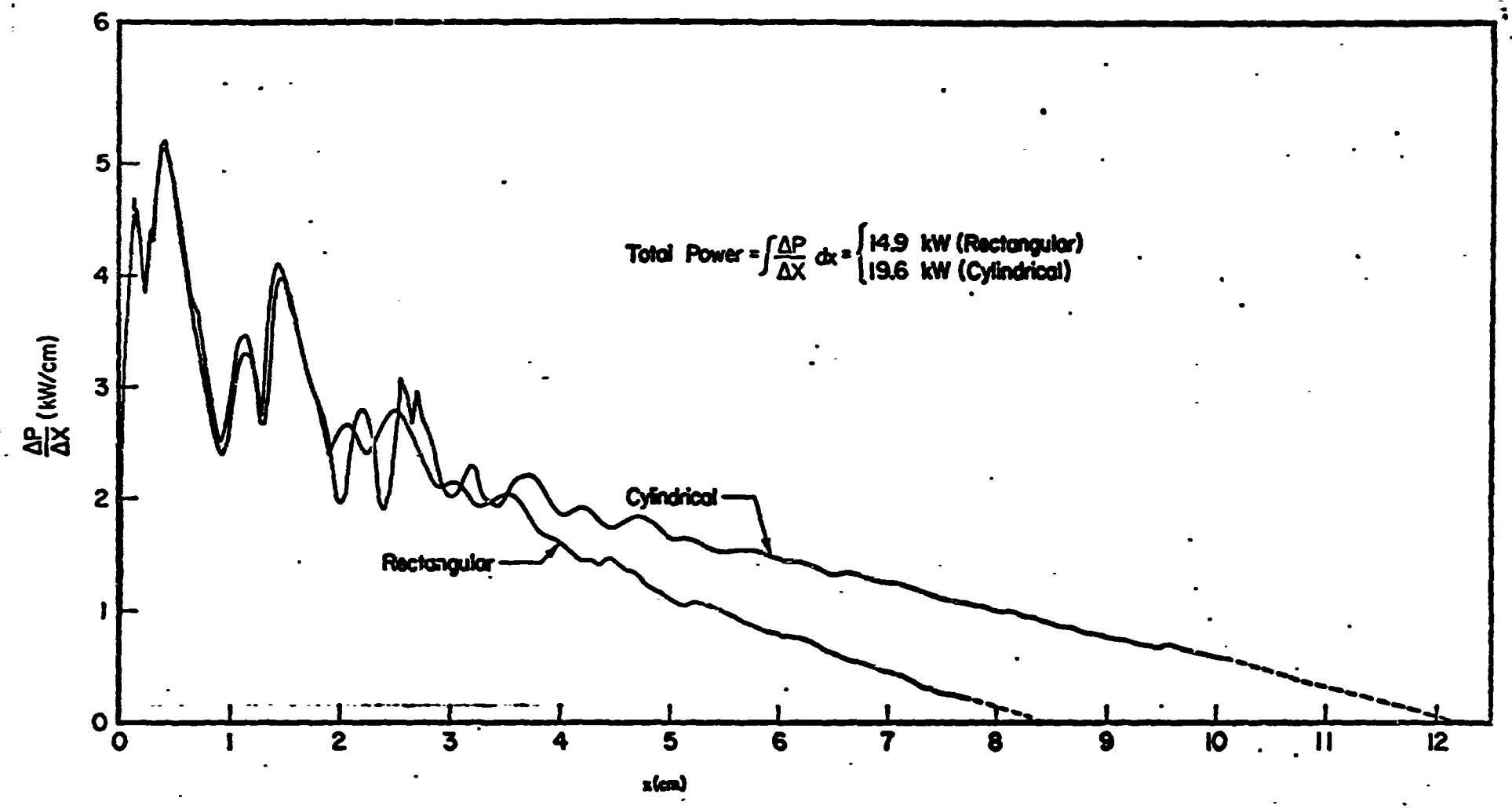

Fig. 10. Rectangular and normalized cylindrical power profiles.

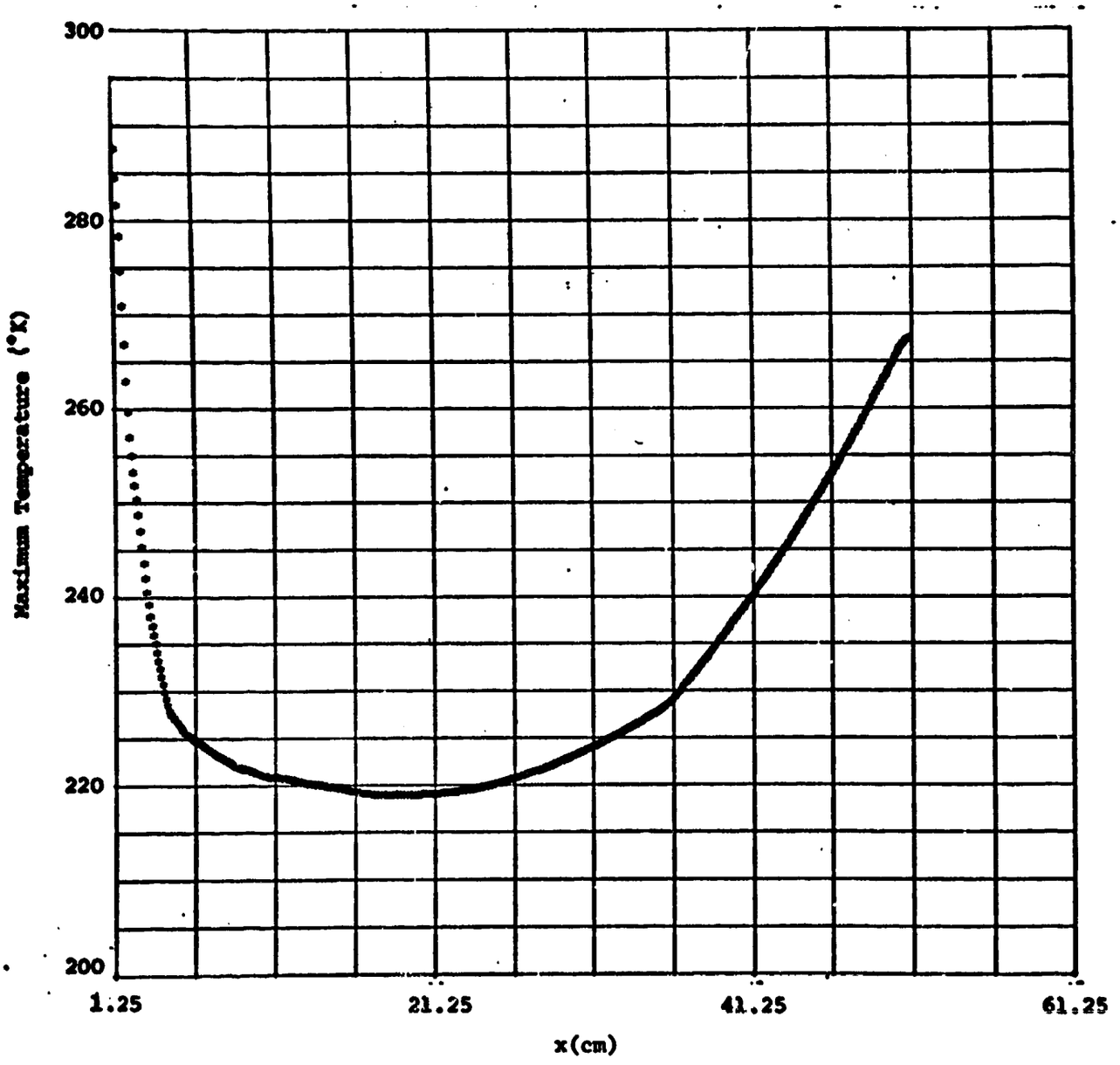

Fig. 11. Plot of maximum temperature vs x for the Rocketdyne baseline chain reaction calculation.

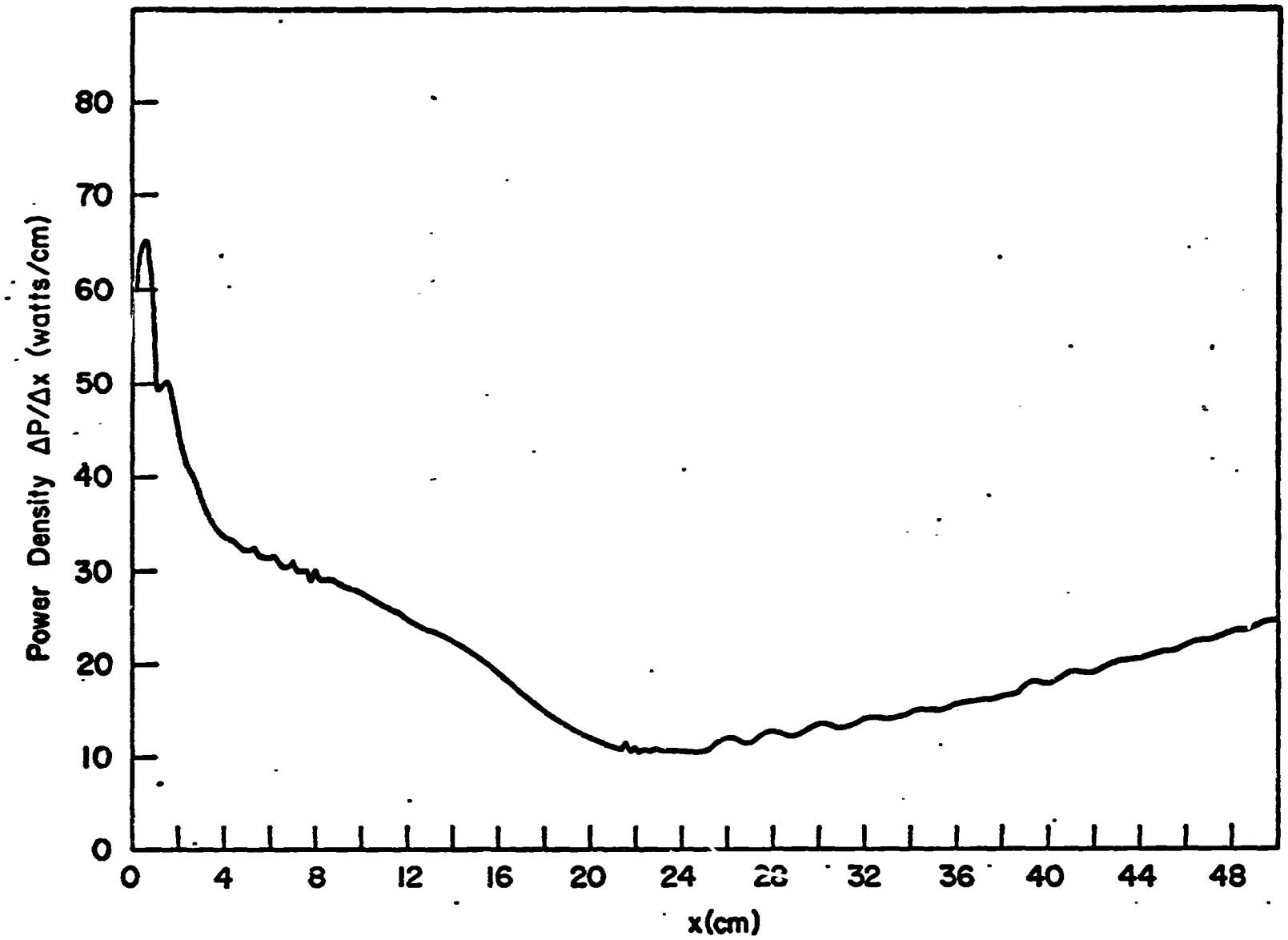

Fig. 12. Power profile for the Rocketdyne baseline chain reaction calculation.